ELECTRONIC SUPPLEMENTARY INFORMATION

Comparative solution equilibrium studies of antitumor ruthenium(η^6-*p*-cymene) and rhodium(η^5-C_5Me_5) complexes of 8-hydroxyquinolines

Orsolya Dömötör, Veronika F.S. Pape, Nóra V. May, Gergely Szakács, Éva A. Enyedy*

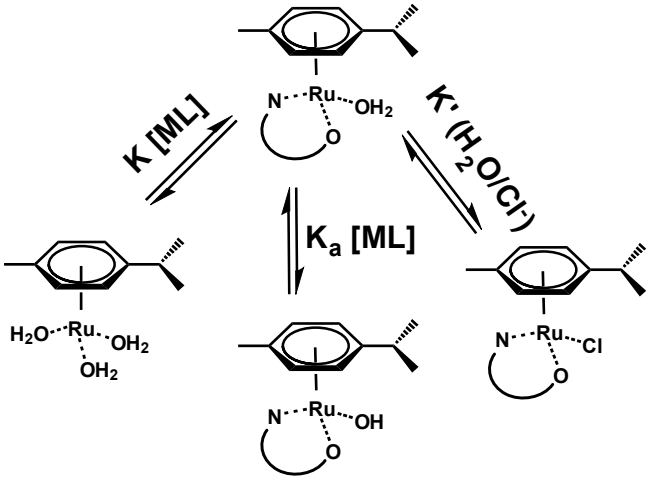

Chart S1. Complex formation, deprotonation and co-ligand (H_2O/Cl^-) exchange equilibrium processes for the [Ru(η^6-*p*-cymene)(L)(H_2O)] species. Charges are omitted for clarity.

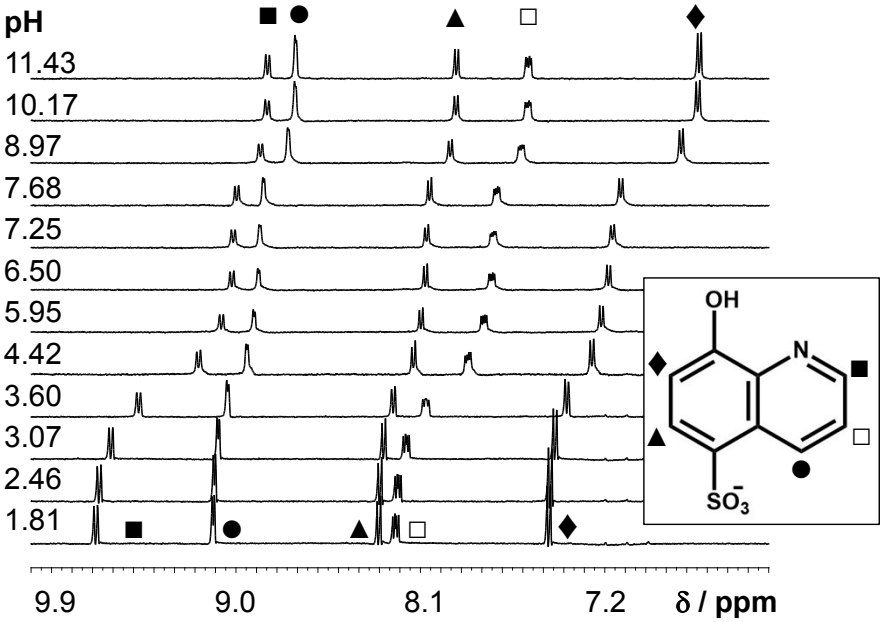

Fig. S1. ^{1}H NMR spectra of the HQS recorded at the indicated pH values with peak assignation. {c_{HQS} *= 1 mM; T = 25 °C; I = 0.20 M (KNO_3); 10% D_2O*}.

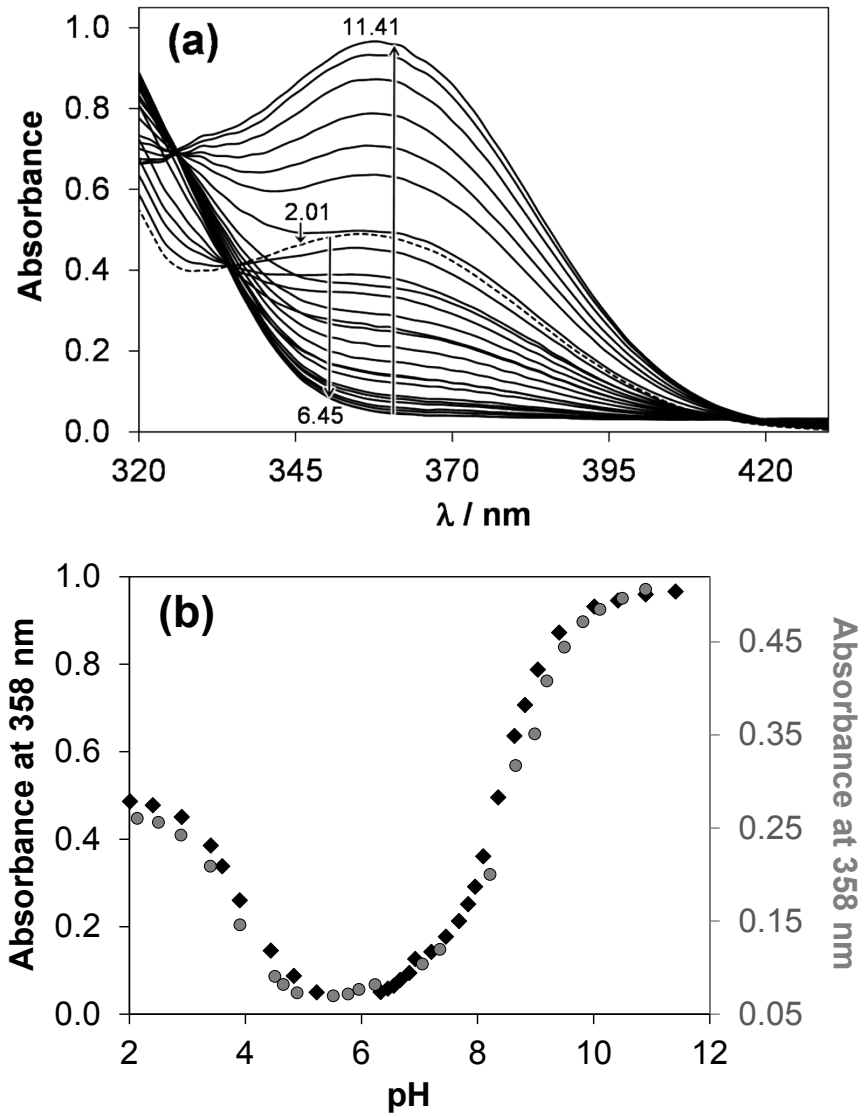

Fig. S2. UV–Vis spectra recorded for HQS (c_L = *1 mM*) at various pH values (pH = 2.0-11.5) (a). Absorbance values at 358 nm at two kinds of ligand concentrations: 1 mM, l = 0.2 cm (♦) and 0.1 mM, l = 1.0 cm (●) plotted against the pH (b) {*T = 25 ˚C; I = 0.20 M (KNO_3)*}.

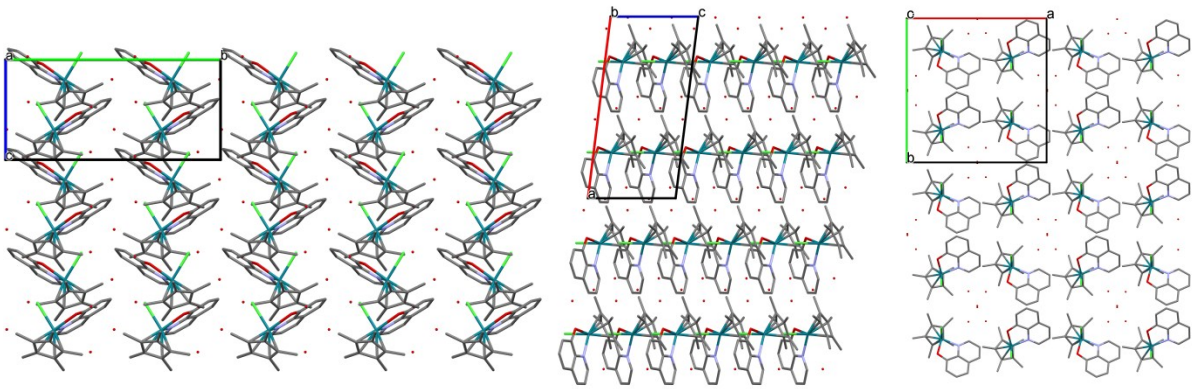

Fig. S3. The crystal packing of complex [Rh(η^5-C_5Me_5)(8-quinolinolato)(Cl)] (**1**) viewed from the *a*, *b* and *c* crystallographic axes, respectively, from left to right. Hydrogen atoms are omitted for clarity.

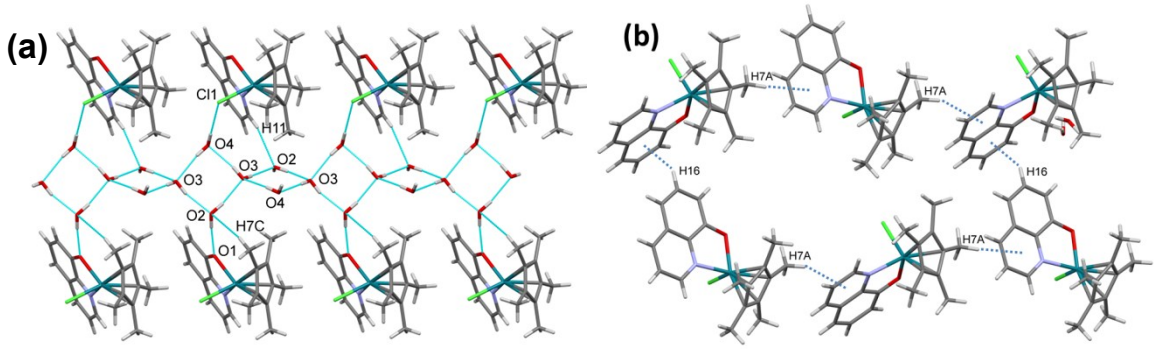

Fig. S4. Packing arrangement in crystal [Rh(η^5-C_5Me_5)(8-quinolinolato)(Cl)] (**1**) showing hydrogen bond connections with water molecules (a) and C–H…π interactions (b). Details of the interactions are listed in Table S2.

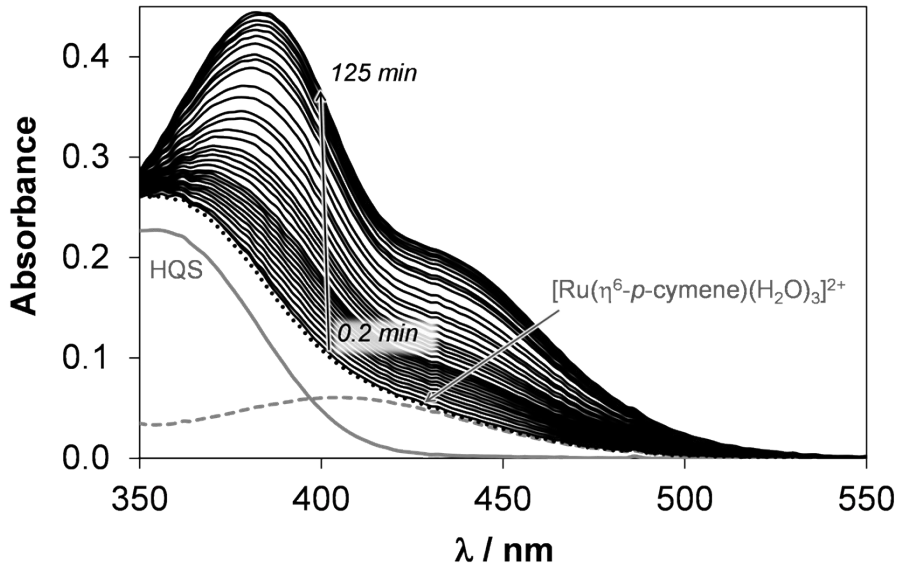

Fig. S5. Time-dependence of the UV–Vis spectra recorded for the $[Ru(\eta^6\text{-}p\text{-cymene})(H_2O)_3]^{2+}$ – HQS (1:1) system at pH 3.0 (black lines) and spectra of the unbound ligand (grey solid line) and the organoruthenium cation (grey dashed line). {*t = 0.2 – 125 min; $c_L = c_{Rh}$ = 99 μM; T = 25 ˚C; I = 0.20 M (KNO_3)*}.

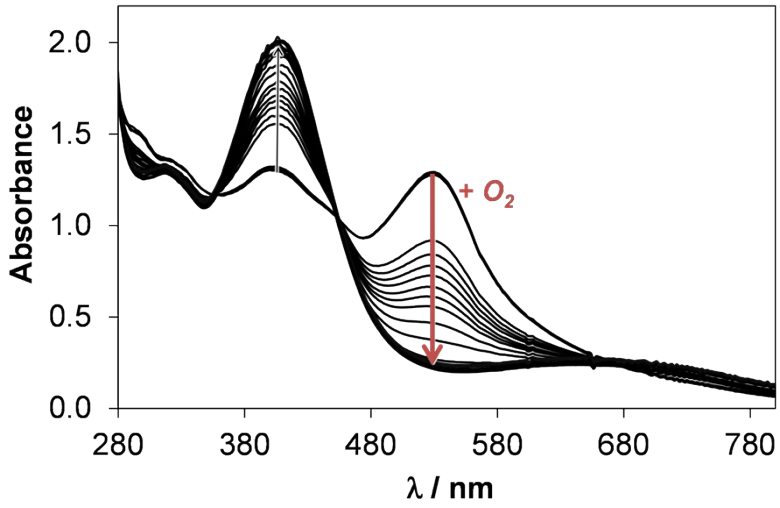

Fig. S6. The effect of oxygen gas on the UV–Vis absorbance spectra of $[Ru(\eta^6\text{-}p\text{-cymene})(H_2O)_3]^{2+}$ – HQS (1:2) system kept under Ar atmosphere beforehand at pH 7.4. {*c_{Ru} = 223 μM; c_{HQS} = 444 μM; pH = 7.4 (20 mM phosphate buffer); T = 25 ˚C*}.

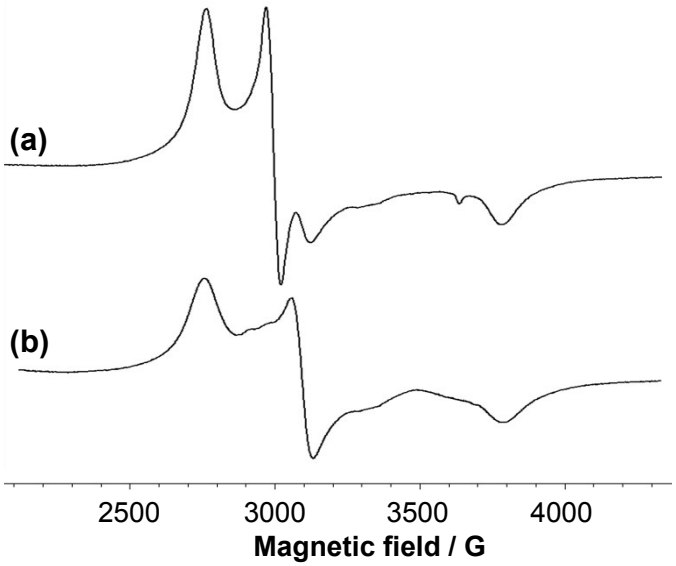

Fig S7. EPR spectra recorded for the $[Ru(\eta^6\text{-}p\text{-cymene})(H_2O)_3]^{2+}$ – HQS (1:2) system under aerobic conditions at pH 11.1 ($g_x = 2.436$, $g_y = 2.246$, $g_z = 1.775$) (a) and pH 7.4 ($g_x = 2.449$, $g_y = 2.174$, $g_z = 1.772$) (b) after 1 day incubation time. {c_{Ru} = *10 mM; T = 77 K*}

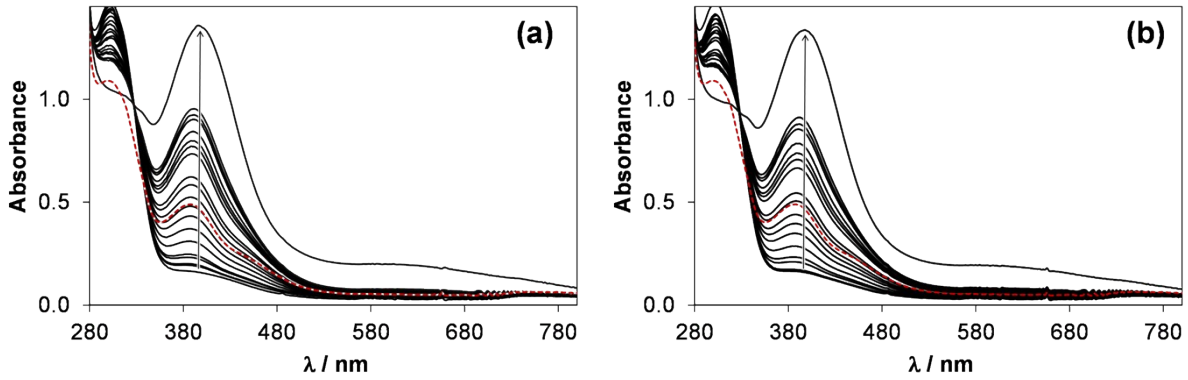

Fig. S8. Time-dependent UV–Vis absorbance spectra of $[Ru(\eta^6\text{-}p\text{-cymene})(H_2O)_3]^{2+}$ – HQ (1:2) system at pH 7.4 under aerobic condition (a) and under Ar atmosphere (b); red dashed spectrum is calculated as sum of $[Ru(\eta^6\text{-}p\text{-cymene})(HQ)(H_2O)]^+$ and 1 eq HQ. {c_{Ru} = *222 μM;* c_L = *445 μM; pH = 7.4 (20 mM phosphate buffer); T = 25 ˚C*}.

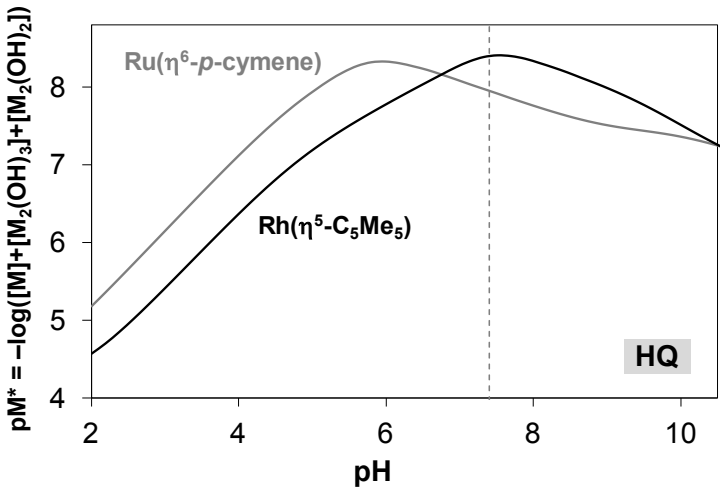

Fig. S9. pH-dependence of pM* values calculated for the $[Rh(\eta^5\text{-}C_5Me_5)(H_2O)_3]^{2+}$ – HQ (black line) and $[Ru(\eta^6\text{-}p\text{-cymene})(H_2O)_3]^{2+}$ – HQ (grey line) systems at 1:1 metal-to-ligand ratio. pM* = –log([M] + $[M_2(OH)_3]$ + $[M_2(OH)_2]$). {*c_M = 50 μM; M:L = 1:1; T= 25 °C; I = 0.20 M (KNO_3)*}.

Table S1

Crystal data and structure refinement parameters for [Rh(η^5-C_5Me_5)(8-quinolinolato)Cl] × $3H_2O$ (**1**) [a]

Compound	**1**
Color/shape	Orange/Block
Empirical formula	$C_{19}H_{27}ClNO_4Rh$
Moiety formula	$[Rh(C_{19}H_{27}NO)(Cl)]\times 3(H_2O)$
Formula weight	471.77
Temperature (K)	103(2)
Radiation and wavelength (Å)	Mo-Kα, λ =0.71073
Crystal system	monoclinic
Space group	*C*c
Unit cell dimensions	
a (Å)	*a* =15.9461(6)
b (Å)	*b* =16.3041(6)
c (Å)	*c* =7.6492(3)
β (°)	β =97.1320(10)
Volume ($Å^3$)	1973.30(13)
Z/*Z'*	4/1
Density (calc.) (Mgm^{-3})	1.588
Absorption coefficient, μ (mm^{-1})	1.024
F(000)	968
Crystal size (mm)	0.50 x 0.12 x 0.12
Absorption correction	Multi-scan
Min. and max. transmission	0.7428 and 1.0000
θ–range for data collection (°)	$3.093 \le \theta \le 27.480$
Index ranges	$-20 \le h \le 20; -21 \le k \le 21; -9 \le l \le 9$
Reflections collected	38253
Completeness to 2θ	0.998
Independent reflections (R_{int})	4470 (0.0447)
Reflections $I>2\sigma(I)$	4300
Refinement method	full-matrix least-squares on F^2
Data / restraints / parameters	4470 /8 /258
Goodness-of-fit on F^2 [b]	1.105
Final *R* indices [$I>2\sigma(I)$] R_1, wR_2 [c]	0.0311, 0.0730
R indices (all data) R_1, wR_2	0.0329, 0.0739
Max. and mean shift/esd	0.001;0.000
Largest diff. peak and hole ($e.Å^{-3}$)	0.857;-0.988

[a] Uncertainties (SD) of the last digits are shown in parentheses.

[b] GOF = $\{\Sigma[w(F_o^2 - F_c^2)^2]/(n-p)\}^{1/2}$, where *n* is the number of reflections and *p* is the total number of parameters refined.

[d] $R_1 = \Sigma||F_o| - |F_c||/\Sigma|F_o|$; $wR_2 = \{\Sigma[w(F_o^2 - F_c^2)^2]/\Sigma[w(F_o^2)^2]\}^{1/2}$

Table S2
Intermolecular interactions in the crystal structure of [Rh(η^5-C_5Me_5)(8-quinolinolato)Cl] × $3H_2O$ (**1**)

D-H…A	D…H (Å)	H…A (Å)	D…A (Å)	D-H…A (°)
O2-H2o…O1	0.86(5)	1.84(5)	2.701(6)	175(9)
O2-H2w…O3^{i}	0.85(7)	1.89(7)	2.734(7)	170(7)
O3-H3o…O4^{ii}	0.84(6)	1.92(6)	2.754(7)	172(5)
O3-H3w…O2	0.84(6)	1.88(6)	2.699(7)	164(6)
O4-H4o…O3^{iii}	0.84(6)	1.95(7)	2.772(7)	167(6)
O4-H4w…Cl1	0.84(4)	2.35(4)	3.191(5)	175(8)
C7-H7c…O2	0.98	2.55	3.523(9)	169
C11-H11…O2^{iv}	0.95	2.58	3.309(8)	134
C7-H7a…Cg(B)^{v}	0.98	3.00	3.907(8)	155
C16-H16…Cg(C)^{i}	0.95	2.73	3.483(7)	137

Symmetry codes:
^{i}x,2-y,1/2+z, ^{ii}-1/2+x,3/2-y,-1/2+z, ^{iii}1/2+x,-1/2+y,z, ^{iv}1/2+x,3/2-y,1/2+z, ^{v}-1/2+x,3/2-y,1/2+z